On the large-scale dynamics of *f*–plane zonally symmetric circulations

Cite as: AIP Advances **9**, 015001 (2019); https://doi.org/10.1063/1.5051737
Submitted: 11 August 2018 . Accepted: 20 December 2018 . Published Online: 02 January 2019

Chanh Kieu, and Quan Wang

On the large-scale dynamics of f−plane zonally symmetric circulations

Cite as: AIP Advances 9, 015001 (2019); doi: 10.1063/1.5051737
Submitted: 11 August 2018 • Accepted: 20 December 2018 •
Published Online: 2 January 2019

Chanh Kieu[1,a] and Quan Wang[2,b]

AFFILIATIONS

[1] Department of Earth and Atmospheric Sciences, Indiana University, Bloomington, Indiana 47405, USA
[2] Department of Mathematics, Sichuan University, Chengdu 610064, China

[a] **Electronic mail:** ckieu@indiana.edu
[b] **Electronic mail:** wqxihujunzi@126.com

ABSTRACT

In this study, an f-plane dynamical model for incompressible flows is presented to examine the mechanisms underlying the structure and stability of large-scale zonally symmetric circulations. Analyses based on the Principle of Exchange of Stabilities reveal that this zonally symmetric model possesses a single-cell structure in the absence of the Coriolis force, similar to the single-cell general atmospheric circulation in the absence of the Earth's rotation as previously hypothesized. The circulation, however, bifurcates into a triple-cell structure in the presence of the Coriolis force if the vertical temperature gradient, the rotational rate, and the momentum eddy coefficients satisfy a certain constraint. Further analyses of this triple-cell structure as a result of the Coriolis force show that this structure is topologically stable, thus offering new insight into the highly resilient structure of the Earth's atmospheric global circulations.

I. INTRODUCTION

The atmosphere is a complex dynamical system. Due to uneven distribution of solar radiation on the Earth's surface that generally decreases with increasing latitudes, the existence of global atmospheric circulations in response to the uneven absorption of the solar radiation at the surface is necessary, which play an important role in maintaining the energy balance between the equator and the poles.[7,9,13,15,21,22,27,39] At the deepest essence, the global circulations can be therefore considered as a direct response of the atmosphere to the warmer temperature at the Earth's surface due to solar heating. Because of the strong dependence of Earth's climate on atmospheric circulations, any changes in the characteristics of atmospheric general circulations will produce large impacts on the Earth's climate and energy transport at both the regional and global scales.

Given the importance of atmospheric circulations in the energy budget and climate, great attention has been paid to elucidating the structure and dynamics of the global atmospheric circulations. In an earlier attempt to understand the steady state of the global circulations, Schneider and Lindzen[38] presented an axially symmetric model in which the large-scale atmospheric motion was assumed to be driven by simple radiative cooling and diabatic heating. Their linearized analyses demonstrated the existence of a circulation that shares some similarity with the observed global circulations. By trying different types of heating profiles, their numerical results also showed that the structure of the circulations in their model largely depends upon the small-scale heat fluxes and the surface frictional force. Following a similar approach, Held and Hou[12] proposed a steady-state axially symmetric model that could demonstrate the factors that most control the variability of the global circulations in a dry stably stratified atmosphere. Their results suggested that the vertical eddy viscosity plays an important role in maintaining the steady structure for the global circulations. A too small momentum eddy viscosity would render large-scale circulations unstable and no steady state could be obtained.

Among the three major cells of the global circulations, the mechanisms underlying the development and stability of the Hadley cell, which is the circulation between the Equator and 30°, are perhaps most extensively studied from both theoretical and modeling perspectives due to its direct thermal nature.[1,2,7,12,14,19,20,27] To obtain some insight into the nature of the Hadley cell, Hart[8] approximated the meridional circulation as a thin band that is differently heated along the horizontal direction in a non-rotating environment. By varying the Prandtl number, he demonstrated that a Hadley-like circulation could develop as a result of different types of instability for different Prandtl number. In a different approach, Lindzen and Hou[20] presented an alternative model for the Hadley cell to examine the seasonal variation of Hadley circulation by adopting asymmetric heating profile centered off the equator. Their study showed that the winter cell is stronger than the summer cell and the intensity of the circulation is very sensitive to the position of the maximum surface temperature. An extension of Lindzen and Hou's study by Hou and Lindzen[14] confirmed that the concentration of the heating seems to play an essential role in the intensity of the global atmospheric circulations. This dominant role of the heating source is however different from that obtained in a study by Pedlosky,[29] which emphasized more on the small-scale turbulent viscosity in maintaining large-scale motions (see Sections IV D and IV F in Pedlosky[29]).

While previous models for the Hadley circulation could demonstrate the role of diabatic heating and turbulent forcings, one notices also from these models the importance of the Earth's rotation in maintaining the global circulations. By improving the steady-state model in Ref. 12, Farrell[7] speculated that the Hadley cell could extend all the way from the equator to the poles in the limit of an inviscid fluid with a sufficiently high Rossby number such that the Coriolis force can be neglected. This single-cell hypothesis of the global circulations in the limit of no Earth's rotation is somewhat similar to the early concept of a general circulation suggested by Hadley.[21] Following Farrell's argument, it can be then inferred that the Hadley cell would be confined in the tropical region if the effect of Coriolis force is taken into account, thus implying the existence of other cells in the midlatitude regions (see Figure 1). Although Farrell's argument is supported by a later numerical study of Walker and Scheneider,[33,35,42] it was nevertheless mostly based on different prescribed heating or moisture functions. As such, it is still unclear why the global circulations are composed of a single cell but not any other number of cells in the absence of the Earth's rotation.

Despite extensive studies in understanding the global atmospheric circulations from various theoretical, modeling, observational, and laboratory perspectives as mentioned above, several fundamental questions related to the structure of these global circulations still remain. Specifically, the mechanisms behind the emergence of the triple-cell structure of the global circulations as well as the related stability of this structure are still not well understood. Using a global climate model, Walker and Scheneider[42] found that the meridional temperature gradient appears to be one of the key factors

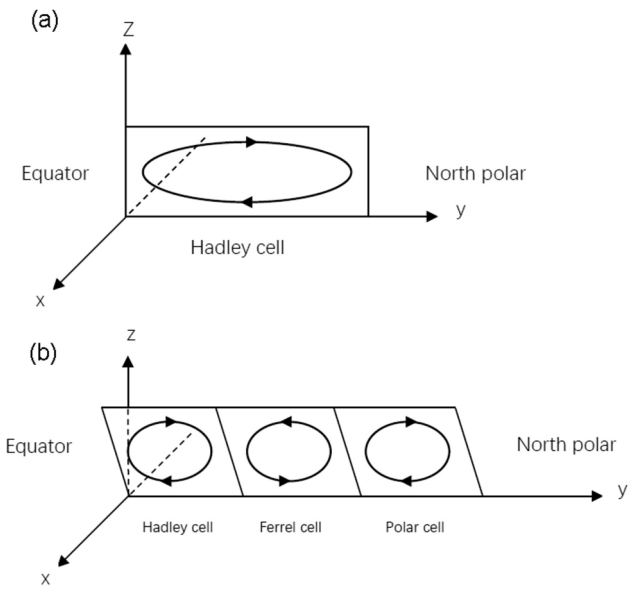

FIG. 1. Schematic illustration of the structure of zonally averaged global atmospheric circulation for (a) a non-rotating Earth, and (b) a rotating Earth, which is based on Farrell (1982)'s model.

in determining the number of cells between the equator and 60° latitude, which could take 1, 3 or 5 cells for temperature difference of 30K, 60 K, and 90K, respectively. It is however not explained why these structures are stable in their modeling study. Moreover, the role of the Earth's rotation in generating specifically three instead of an arbitrary number of cells is still elusive, other than evidence from their numerical experiments.

Recent progress in the transition dynamics for dissipative systems developed by Ma and Wang[23–25] offers a framework to tackle the large-scale circulation from a different angle. Unlike the traditional linear stability analyses, the transition dynamical theory examines conditions for which a dynamical system bifurcates from one stable configuration to the next as model parameters change. Given these progresses in nonlinear dynamics, the objective of this study is to examine the dynamics of zonally symmetric circulations (ZSC) in an incompressible flow that could mimic the Earth's global circulations. Our specific focus will be on understanding the structure and related stability of the ZSCs as a natural consequence of the Principle of Exchange of Stabilities (PES), which determines the bifurcation of the Navier-Stokes equations. While our ZSC model proposed in this study is certainly far from the real atmosphere, it is our aim to examine to what extent this ZSC model can offer any insight into the structure and stability of the atmospheric triple-cell circulation, and how this structure changes in the presence and in the absence of the Earth's rotation.

In the next, a model for ZSCs will be presented. Analyses of the bifurcation characteristics for this ZSC model in the absence and in the presence of the Coriolis force will be then

discussed in Section II. Section III examines the stability of the new ZSC structures as a result of the dynamical transition, and concluding remarks as well as shortcomings of our ZSC model are discussed in the final section.

II. A ZONALLY SYMMETRIC CIRCULATION MODEL

A. Formulation

Given the unique symmetric nature of the global atmospheric circulations in the meridional plane (y, z), we will follow previous studies and model ZSCs as a two-dimensional (2D) rotating Boussinesq fluid in the meridional-height plane (y, z) as follows:[1,2,8,12]

$$\begin{aligned}
&\frac{\partial u}{\partial t} + (\mathbf{u}\cdot\nabla)u = fv + \nu_1\frac{\partial^2 u}{\partial y^2} + \nu_2\frac{\partial^2 u}{\partial z^2},\\
&\frac{\partial v}{\partial t} + (\mathbf{u}\cdot\nabla)v = -\frac{1}{\rho_0}\frac{\partial P}{\partial y} - fu + \nu_1\frac{\partial^2 v}{\partial y^2} + \nu_2\frac{\partial^2 v}{\partial z^2},\\
&\frac{\partial w}{\partial t} + (\mathbf{u}\cdot\nabla)w = -\frac{1}{\rho_0}\frac{\partial P}{\partial z} + \frac{g\theta}{\theta_0} + \nu_1\frac{\partial^2 w}{\partial y^2} + \nu_2\frac{\partial^2 w}{\partial z^2}, \qquad (2.1)\\
&\frac{\partial \theta}{\partial t} + (\mathbf{u}\cdot\nabla)\theta = \kappa_1\frac{\partial^2 \theta}{\partial y^2} + \kappa_2\frac{\partial^2 \theta}{\partial z^2} + Q,\\
&\frac{\partial v}{\partial y} + \frac{\partial w}{\partial z} = 0,
\end{aligned}$$

where $\mathbf{u} \equiv (u, v, w)$ are the wind components in the zonal, meridional and vertical directions, f is Coriolis parameter, H is the scale height of the troposphere, P denotes the pressure perturbation relative to a reference pressure, ρ_0 is density of the fluid, θ is reference temperature, Q is net diabatic heating per unit mass, (ν_1, ν_2) are horizontal and vertical eddy viscosity coefficients, and (κ_1, κ_2) are horizontal and vertical diffusion coefficients. In this 2D model, the atmosphere is defined as a rectangle domain of the size $[0, L] \times [0, H]$, where L and H are the horizontal and vertical scales of the atmosphere, respectively. Note also that because of the zonally symmetric assumption, all variables are functions of (y, z) only, and so $\mathbf{u}\cdot\nabla \equiv v\partial_y + w\partial_z$.

Unlike the previous Hadley cell models in which either the momentum eddy viscosity coefficients were assumed to be the same in both horizontal and vertical directions or only vertical eddy viscosity was considered, one notices in our governing system (2.1) however that two different coefficients for the momentum eddy viscosity are assumed similar to those in Pedlosky's model (see Chapter 4[29]). The justification for this consideration is based on the fact that the Earth's general atmospheric circulation is inherently governed by strong eddy fluxes such that both horizontal and vertical fictional forces are important.[10,11,21,39] Given the drastically different vertical and horizontal scales of the general atmospheric circulations, it is apparent that the equal contribution of these two eddy terms, i.e. $\nu_1\frac{\partial^2 u}{\partial y^2} \sim \nu_2\frac{\partial^2 u}{\partial z^2}$ can be held only if $\nu_1 \neq \nu_2$. Such a difference between the vertical and horizontal eddy coefficients is observed in the real atmosphere conditions. Estimations of these coefficients in previous studies[16,29] showed that $\nu_1 \sim 10^3 - 10^5 m^2\ s^{-1}$, whereas $\nu_2 \sim 10^{-1} - 10^{-4} m^2\ s^{-1} \ll -Nu_1$. This difference between the horizontal and vertical momentum eddy coefficients has an important implication on the transition dynamics as will be seen in the next section.

We note here that the use of a rotating incompressible fluid on a rectangle domain to represent the large-scale atmospheric circulations in (2.1) has some inherent drawbacks, as the real atmosphere is compressible and the Coriolis force is not a constant but varies with latitudes. While the compressibility issue can be overcome by some coordinate transformations or use of the anelastic approximation, the assumption of a constant Coriolis force is admittedly rough, as the constant Coriolis force is more suitable for laboratory experiments than for the actual atmosphere.[15] Inspired by numerous laboratory studies and theoretical works on the stability of the Hadley circulation using simplified models similar to (2.1), our main attempt in this study is thus limited to examining the main properties of the ZSC on an f−plane, i.e., how much of the zonally symmetric atmospheric circulation can be explained by the f-plane dynamics. The use of the f−plane dynamics is certainly a caveat of (2.1) in describing the atmospheric global circulations, but on the other hand anticipated due to the complexity of the atmosphere. As emphasized by Lorenz,[21] a complete description of the general atmospheric circulations would seem to be impractical from the theoretical perspective, because any analytical research can only be applied to one or two specific aspects of the atmospheric circulations rather than for the entire atmosphere. With this caveat in mind, we will limit our focus on how much of the ZSC dynamics that we can learn from Eq. (2.1), which we now turn into.

B. A reduced model

The most challenging question that one has to first address is how to realistically represent the net diabatic heating rate Q in our ZSC model (2.1). This is a very difficult problem because this heating rate composes of various physical processes that are currently not fully understood such as radiative transfer, cloud physics, atmospheric gas concentration, aerosol, or phase transition. Indeed, these processes are so complex that it is unlikely, if at all possible, to find any functional form for the term heating Q.[8,12,20,21,32] As a result, many previous models of the general atmospheric circulations often assumed a simplified form for the diabatic heating such as $Q = (\theta_E - \theta)/\tau$, where θ_E is a given temperature structure established by the radiative-convective equilibrium that the atmosphere must relax to, and τ is the relaxation time.[7,12,20,38]

While a complete representation of this net heating term is beyond our current knowledge, it happens in nature that Q is dominated by latent heat release and radiative cooling in the tropical troposphere.[9,12,13,18,20,26] On average, the net heating rate tends to be negative in the subtropical region due to the dominance of the radiative cooling, and positive in the tropical region due to the dominance of the latent heating. These patterns of the large-scale heating and cooling turn out

to be consistent with the large-scale structure of the vertical motion associated with the general atmospheric circulations. Specifically, the vertical motion is ascending in the tropical region where net heating is positive due to the dominance of the latent heating and is descending in the subtropical region where the net heating is negative due to the dominance of radiative cooling.

Given this consistency between the net heating rate and the large-scale vertical motion, we consider a simplified parameterization for the diabatic heating Q in our ZSC model as follows

$$Q = \zeta w, \tag{2.2}$$

where ζ is a proportional coefficient that determines the water phase transition or cooling rate. With the typical large-scale vertical motion $w \sim 10^{-2}\ m\ s^{-1}$, and corresponding changes of temperature in the order of $1K\ day^{-1}$,[18] the magnitude of the proportional constant ζ is $\sim 10^{-4}\ K\ m^{-1}$ for the large-scale circulation. The parameterization (2.2) may look at first similar to the so-called the conditional instability of second kind (CISK) feedback process first proposed by Charney and Elliassen[4,17] in tropical cyclone research. That is, a stronger vertical motion would promote more latent heating, thus resulting in the dominance of the latent heat release in the atmosphere and warming the atmosphere up. Note however that the parameterization (2.2) by no means implies that latent heat is the sole driving force of the general atmospheric circulations as in the original CISK mechanism. This is because (2.2) also allows for the dominance of radiative cooling in the descending region that the original CISK mechanism does not contain, i.e., a descending motion would correspond to the dominance of radiative cooling and/or evaporative cooling that tends to decrease the overall temperature. As a result of this heating parameterization, a meridional temperature gradient would emerge such that the atmospheric circulation can develop.

Although the above CISK-like diabatic heating parameterization differs from the previous radiative-adjustment approximations and apparently naive for the real atmosphere,[6] it could at least capture the main features related to the large-scale diabatic heating and temperature gradient in a broader global circulation context as discussed in Refs. 28 and 32. We should mention at this point that the use of a more popular radiative-adjustment parameterization for the diabatic heating term Q that relaxes towards a given radiative-convective state θ_E as $Q = (\theta_E - \theta)/\tau$ proposed in Refs. 7 and 12 only changes the structure of the mean flow, but not the characteristics of the transition dynamics (see the eigenvalue problem (3.3) below). This radiative-adjustment parameterization, however, introduces some complication related to the dependence of the eigenvalues on z, which requires numerical procedures and so not presented herein. Because of our main focus in this work is on a dynamical model for idealized ZSC model, this simplified diabatic heating parameterization should be considered as a property of our ZSC model, rather than the actual diabatic heating in the general atmospheric circulations.

With the above representation for the net heating rate Q, it is immediate to see that the system (2.1) admits a simple steady state as follows

$$\mathbf{u}_c = (0,0,0), \theta_c = \theta_1 - \frac{(\theta_1 - \theta_2)z}{H}. \tag{2.3}$$

where θ_1 and θ_2 are the temperature at $z = 0$ and $z = H$. This steady state is unique, and it strictly has no motion in any direction (i.e., a completely quiescent atmosphere) with the temperature gradient purely in the vertical direction. One notices that this steady state is y-independent and so it does not represent the actual physical state of the atmosphere. It is simply a steady state of the governing system (2.1). Our goal is to show that this steady state is unstable, thus allowing for the dynamical transition process that produces a more realistic structure of the general atmospheric circulations as will be shown below (see (3.20) and (3.21)).

To achieve this goal, we consider next a perturbation added to the steady state (2.3) and examine conditions for which the dynamical transition can take place. Assume the perturbation under consideration is zonally symmetric such that $\frac{\partial}{\partial x} = 0$, the flow vectors and temperature can be written as

$$\mathbf{u} = \mathbf{u}_c + \mathbf{u}', \theta = \theta_c + \theta'. \tag{2.4}$$

Plugging these perturbations into (2.1) leads to

$$\begin{aligned}
&\frac{\partial u}{\partial t} + (\mathbf{u}\cdot\nabla)u - fv = \nu_1\frac{\partial^2 u}{\partial y^2} + \nu_2\frac{\partial^2 u}{\partial z^2},\\
&\frac{\partial v}{\partial t} + (\mathbf{u}\cdot\nabla)v + fu = \nu_1\frac{\partial^2 v}{\partial y^2} + \nu_2\frac{\partial^2 v}{\partial z^2} - \frac{1}{\rho_0}\frac{\partial P}{\partial y},\\
&\frac{\partial w}{\partial t} + (\mathbf{u}\cdot\nabla)w = \nu_1\frac{\partial^2 w}{\partial y^2} + \nu_2\frac{\partial^2 w}{\partial z^2} - \frac{1}{\rho_0}\frac{\partial P}{\partial z} + g\frac{\theta}{\theta_0},\\
&\frac{\partial \theta}{\partial t} + (\mathbf{u}\cdot\nabla)\theta - \frac{(\theta_1 - \theta_2)w}{H} = \kappa_1\frac{\partial^2 \theta}{\partial y^2} + \kappa_2\frac{\partial^2 \theta}{\partial z^2} - \zeta w,\\
&\frac{\partial v}{\partial y} + \frac{\partial w}{\partial z} = 0,
\end{aligned} \tag{2.5}$$

where the primes have been dropped for convenience. We next introduce a set of scales

$$\begin{aligned}
&(y,z) = H(y^*,z^*), \quad t = \frac{H^2}{\kappa_2}t^*, \quad \mathbf{u} = \frac{\kappa_2}{H}\mathbf{u}^*,\\
&P = \frac{\rho_0\kappa_2^2}{H^2}P^*, \quad \theta = (\theta_1 - \theta_2)\theta^*,
\end{aligned} \tag{2.6}$$

where the asterisks denote nondimensional variables. If one notes further that the continuity equation in (2.5) allows us to define a stream function ψ such that $(v*, w*)$ can be given by

$$\left(\frac{\partial \psi}{\partial z}, -\frac{\partial \psi}{\partial y}\right),$$

(2.5) can be then written in nondimensional forms as

$$\begin{aligned}
&\frac{\partial u}{\partial t} - \mathrm{J}(\psi, u) - \mathrm{T}\frac{\partial \psi}{\partial z} = \mathrm{P}_r\left(\mathrm{E}\frac{\partial^2 u}{\partial y^2} + \frac{\partial^2 u}{\partial z^2}\right),\\
&\frac{\partial \Delta\psi}{\partial t} - \mathrm{J}(\psi, \Delta\psi) + \mathrm{T}\frac{\partial u}{\partial z} = \mathrm{P}_r\left(\mathrm{E}\frac{\partial^2 \Delta\psi}{\partial y^2} + \frac{\partial^2 \Delta\psi}{\partial z^2}\right) - \mathrm{R}\frac{\partial \theta}{\partial y},\\
&\frac{\partial \theta}{\partial t} - \mathrm{J}(\psi, \theta) + \frac{\partial \psi}{\partial y} = \mathrm{K}\frac{\partial^2 \theta}{\partial y^2} + \frac{\partial^2 \theta}{\partial z^2} + \mathrm{B}\frac{\partial \psi}{\partial y}.
\end{aligned} \tag{2.7}$$

where the asterisks are dropped for the sake of notation, $\mathrm{J}(\psi,\varphi) = \frac{\partial \psi}{\partial y}\frac{\partial \varphi}{\partial z} - \frac{\partial \psi}{\partial z}\frac{\partial \varphi}{\partial y}$ for the state $\varphi \equiv (u, \psi, \theta)$, and the nondimensional parameters B, E, T, K, R, and P_r in (2.7) are defined as follows

$$\begin{aligned}
&\mathrm{E} = \frac{\nu_1}{\nu_2}, \mathrm{K} = \frac{\kappa_1}{\kappa_2},\\
&\mathrm{T} = \frac{f\mathrm{H}^2}{\kappa_2}, \mathrm{R} = \frac{g\mathrm{H}^3(\theta_1 - \theta_2)}{\theta_0 \kappa_2^2}, \mathrm{B} = \frac{\zeta \mathrm{H}}{\theta_1 - \theta_2} < 1,\\
&\mathrm{P}_r = \frac{\nu_1}{\kappa_1} = \frac{\nu_2}{\kappa_2}.
\end{aligned}$$

Among these several parameters, we note that R is the Rayleigh number, and the turbulent Prandtl number P_r is typically ~ 1 for the atmospheric flows, which will be herein assumed for both the vertical and horizontal directions.[1,2,12,14,20,29] The effects of diabatic heating is incorporated in the nondimensional B number.

Under the scaling given by (2.6), the domain for (2.7) is thus reduced to

$$\Omega = (0, a) \times (0, 1), \text{ where } a \equiv \frac{\mathrm{L}}{\mathrm{H}}$$

to which the following boundary conditions will be imposed

$$\begin{aligned}
&u(0,z) = \psi(0,z) = u(a,z) = \psi(a,z) = 0,\\
&\frac{\partial \theta}{\partial y}(0,z) = \frac{\partial \theta}{\partial y}(a,z) = 0,\\
&\frac{\partial u}{\partial z} = \theta = \frac{\partial^2 \psi}{\partial z^2} = \psi = 0, z = 0, 1,
\end{aligned} \tag{2.8}$$

Physically, the boundary conditions (2.8) imply that the wind is non-slip in the y-direction, and it is free on the upper boundary. More detailed discussion about this type of boundary conditions can be found, e.g., in Ref. 12.

III. TRANSITION DYNAMICS

A. Eigenvalue problem

To facilitate our analyses, we first re-write (2.7) in terms of differential operators as follows

$$\frac{d\varphi}{dt} = \mathcal{A}^{-1}\mathrm{L}\varphi + \mathcal{A}^{-1}\mathrm{G}\varphi. \tag{3.1}$$

where the operators $\mathcal{A}$, L, and G are defined as

$$\begin{aligned}
\mathcal{A}\varphi &= \begin{pmatrix} u \\ \Delta\psi \\ w \end{pmatrix},\\
\mathrm{L}\varphi &= \begin{pmatrix} \mathrm{P}_r\left(\mathrm{E}\frac{\partial^2 u}{\partial y^2} + \frac{\partial^2 u}{\partial z^2}\right) + \mathrm{T}\frac{\partial \psi}{\partial z} \\ \mathrm{P}_r\left(\mathrm{E}\frac{\partial^2 \Delta\psi}{\partial y^2} + \frac{\partial^2 \Delta\psi}{\partial z^2}\right) - \mathrm{R}\frac{\partial \theta}{\partial y} - \mathrm{T}\frac{\partial u}{\partial z} \\ \mathrm{K}\frac{\partial^2 \theta}{\partial y^2} + \frac{\partial^2 \theta}{\partial z^2} - (1-\mathrm{B})\frac{\partial \psi}{\partial y} \end{pmatrix},\\
\mathrm{G}\varphi &= \begin{pmatrix} \mathrm{J}(\varphi, u) \\ \mathrm{J}(\varphi, \Delta\psi) \\ \mathrm{J}(\varphi, w) \end{pmatrix}.
\end{aligned} \tag{3.2}$$

The operator form of (2.7) brings a lot of convenience in deriving the corresponding transition number as will be shown below. Following the standard procedures, the eigenvalue problem for the linear differential operators in (2.7) is then given by:

$$\begin{aligned}
&\mathrm{P}_r\left(\mathrm{E}\frac{\partial^2 u}{\partial y^2} + \frac{\partial^2 u}{\partial z^2}\right) + \mathrm{T}\frac{\partial \psi}{\partial z} = \lambda u,\\
&\mathrm{P}_r\left(\mathrm{E}\frac{\partial^2 \Delta\psi}{\partial y^2} + \frac{\partial^2 \Delta\psi}{\partial z^2}\right) - \mathrm{R}\frac{\partial \theta}{\partial y} - \mathrm{T}\frac{\partial u}{\partial z} = \lambda \Delta\psi,\\
&\mathrm{K}\frac{\partial^2 \theta}{\partial y^2} + \frac{\partial^2 \theta}{\partial z^2} - (1-\mathrm{B})\frac{\partial \psi}{\partial y} = \lambda\theta,
\end{aligned} \tag{3.3}$$

for a general eigenvalue λ along with boundary conditions (2.8). It can be directly verified that for the eigenvalue problem (3.3) a general eigenvector must have the following form,

$$\begin{aligned}
u &= \mathrm{U}(z)\sin b_m y,\\
\psi &= \mathrm{V}(z)\sin b_m y,\\
\theta &= -\mathrm{W}(z)\cos b_m y,
\end{aligned} \tag{3.4}$$

where $b_m = \frac{m\pi}{a}, m \in \mathrm{Z}$, and U(z), V (z) and W(z) satisfy the following relationships

$$\begin{aligned}
&\mathrm{P}_r\left(\mathrm{D}^2 - \mathrm{E}b_m^2\right)\mathrm{U} + \mathrm{TDV} = \lambda \mathrm{U},\\
&\mathrm{P}_r\left(\mathrm{D}^2 - \mathrm{E}b_m^2\right)(\mathrm{D}^2 - b_m^2)\mathrm{V} - \mathrm{R}b_m\mathrm{W} = \lambda(\mathrm{D}^2 - b_m^2)\mathrm{V} + \mathrm{TDU},\\
&\left(\mathrm{D}^2 - \mathrm{K}b_m^2\right)\mathrm{W} + (1-\mathrm{B})b_m\mathrm{V} = \lambda \mathrm{W},\\
&\text{Boundary conditions: } \mathrm{U}' = \mathrm{V} = \mathrm{V}'' = \mathrm{W} = 0, z = 0, 1.
\end{aligned} \tag{3.5}$$

where $\mathrm{D} \equiv d/dz$, and the primes in the boundaries for (3.5) now denote the derivative with respect to z. Using the boundary conditions $\mathrm{U}' = \mathrm{V} = \mathrm{V}'' = \mathrm{W} = 0$, at $z = 0, 1$, it can be seen from (3.5) that this system must contain only even order derivatives of V, i.e.,

$$\mathrm{V} = \mathrm{V}'' = \mathrm{V}^{(4)} = \mathrm{V}^{(6)} = \cdots = 0, z = 0, 1. \tag{3.6}$$

As a result, the solution to (3.5) must be of the form

$$\mathrm{V}_m = \mathrm{A}\sin n\pi z, \tag{3.7}$$

where A is any nonzero constant. Substituting (3.7) into (3.5) gives

$$U(z) = \frac{ATn\pi}{P_r\left(n^2\pi^2 + Eb_m^2\right) + \lambda}\cos(n\pi z). \tag{3.8}$$

$$W(z) = \frac{A(1-B)b_m}{n^2\pi^2 + Eb_m^2 + \lambda}\sin(n\pi z) \tag{3.9}$$

Inserting (3.7)-(3.9) into the second equation of (3.5) and assuming that the Prandtl number $P_r \sim 1$, one obtains a characteristic equation for the eigenvalue λ as follows

$$\lambda = -\frac{F_{m,n}}{2} \pm \sqrt{\frac{F_{m,n}^2}{4} + \frac{P_r R(1-B)b_m^2 - T^2n^2\pi^2}{P_r A_{m,n}} - P_r G_{m,n}^2}, \tag{3.10}$$

where

$$G_{m,n} = \left(n^2\pi^2 + Eb_m^2\right),$$
$$F_{m,n} = (P_r + 1)G_{m,n},$$
$$A_{m,n} = (n^2\pi^2 + b_m^2).$$

The eigenvalues given by (3.10) imposes several important constraints. First, these eigenvalues always have a real part $-F_{m,n}/2 < 0$ by definition of the function $F_{m,n}$. Thus, (3.1) will not contain any dynamical transition if the square root in the eigenvalue (3.10) has a complex value, because a complex value would imply that the steady state (2.3) is always stable. Second, the eigenvalues given by (3.10) are a smooth function of the parameter R with one class of values (the plus sign) increasing with R and the other class (the minus sign) decreasing with R. As a result, it is possible to order all eigenvalues based on the real part of the eigenvalues as follows

$$\cdots \mathrm{Re}[\lambda_n] < \cdots < \mathrm{Re}[\lambda_3] < \mathrm{Re}[\lambda_2] < \mathrm{Re}[\lambda_1].$$

Because the complex eigenvalues will always imply a stable state, this order will be of most interest when the first eigenvalue λ_1, whose sign determines the local stability of the steady-state (2.3), crosses a zero value. To analyze the transition and associated stability of the steady-state (2.3), it is therefore necessary to derive a condition for which the first eigenvalue λ_1 changes its sign, which is presented in the next section.

B. Principle of exchange of stabilities

The expression for the eigenvalues as given by (3.10) allows us to examine a subtle behavior, the so-called dynamical transition process. Unlike the traditional bifurcation that only focuses on the number of model states as the model parameter varies, the dynamical transition is more general because it not only allows for studies of the transition from one state to another but also determines whether the bifurcated states are physical or not even when the number of model states does not change. In this regard, one notices first from the expression (3.10) for the eigenvalues that there exists indeed a particular set of parameters that allow for a dynamical transition from one state to another state as described by the PES condition. Mathematically, the PES condition for a dynamical system is given by the following two requirements:[23–25]

$$i.\begin{cases} \mathrm{Re}[\lambda_1] < 0, & R < R_0, \\ \mathrm{Re}[\lambda_1] = 0, & R = R_0, \\ \mathrm{Re}[\lambda_1] > 0, & R > R_0. \end{cases}$$
$$ii. \quad \lambda_n < 0, \quad R = R_0 \quad \forall n \geq 2. \tag{3.11}$$

Depending on the nondimensional numbers B, T, E, and P_r, there may exist a critical number R_0 and an integer $m \geq 1$ such that the PES condition for the governing system (2.1) can be satisfied. Indeed, a quick examination of (3.10) shows that this number R_0 is given by

$$R_0 = \min_{m\geq 1, n=1} \frac{P_r^2 G_{m,n}^2 A_{m,n} + T^2 n^2 \pi^2}{P_r(1-B)b_m^2} = \min_{m\geq 1} \frac{P_r^2 G_{m,1}^2 A_{m,1} + T^2\pi^2}{P_r(1-B)b_m^2}, \tag{3.12}$$

where we have used the fact that the eigenvalue λ as given by (3.10) is a monotonically increasing function of n such that the search for the minimum in (3.12) is sufficiently applied for $n = 1$. It is readily seen that R_0 satisfies the PES condition (3.11) as expected, which determines when the dynamical transition of (2.1) will occur.

Evaluation of the minimum of (3.12) shows that the critical value R_0 will correspond to a value of b_m^2 given as follows (see Appendix A)

$$b_m^2 \approx \sqrt{\frac{P_r^2\pi^4 + T^2}{P_r^2(E^2 + 2E)}}. \tag{3.13}$$

This is a remarkable result, because it dictate how the number of cells of the ZSC is determined by several parameters including the Coriolis force f (or T), the turbulent Prandtl number P_r, and the ratio of the momentum eddy coefficients E. To see in more details the implication of this result, we recall from the definition of b_m that the integer number m represents the meridional wavenumbers; a value $m = 1$ would correspond to a single-cell circulation from the equator to the pole, while $m = 3$ would correspond to a three-cell structure. Also, the impact of the Earth's rotation is represented by the nondimensional number $T = fH^2/\kappa_2$, which is equal to zero in the absence of the Earth rotation, i.e., $T = 0$ for $f = 0$.

Let m_f and m_0 represent the wavenumbers for the ZSC in the presence and in the absence of the Coriolis force, respectively. We then have

$$\frac{b_{m_f}^2}{b_{m_0}^2} \approx \sqrt{1 + \frac{T^2}{\pi^4}}. \tag{3.14}$$

Taking the Prandtl number $P_r \equiv \frac{\nu_2}{\kappa_2} \sim 1$ and assuming other typical scales in the atmosphere including[13]

$$H \sim 10\ km, \quad f \sim 10^{-5}\ s^{-1},$$
$$\nu_2 \sim 10\ m^2 s^{-1}, \quad L \sim 6400\ km.$$

we thus obtain

$$m_f \approx 3m_0. \tag{3.15}$$

Literally, the relationship (3.15) indicates that the number of meridional cells in the presence of the Earth's rotation is about three times the number of cells in the absence of the Earth's rotation. This remarkable result clearly highlights the profound role of the Coriolis force in determining the structure of the ZSC similar to what obtained from previous modeling studies,[7,42] which is obtained here as a direct consequence of the PES condition under the zonally symmetric configuration.

Further estimation of the wavenumber m_0, using (3.13) and assuming a ratio of the horizontal eddy coefficient over the vertical eddy coefficient $E \equiv \frac{\nu_1}{\nu_2} \sim 4 \times 10^5$ gives

$$m_0 = \frac{L}{H\sqrt{E^2 + 2E}} \sim 1. \tag{3.16}$$

This estimation reveals an intriguing feature that the Earth's large-scale atmospheric circulation appears to support only one cell structure in the meridional plane in the absence of the Coriolis force as speculated by Ref. 7. In the presence of the Earth's rotation, the number of cells is therefore equal to three as a result of the consistency among vertical and horizontal eddy viscosity, the Coriolis parameter, and the spatial scales of the atmosphere as dictated by (3.14). Among these scales, the role of the momentum eddy coefficients $E = \nu_1/\nu_2 \sim 10^5$ is somewhat least expected, as it is often assumed in most idealized fluid dynamical systems that this ratio is equal to one, i.e. $\nu_1 = \nu_2$, based on the homogeneity of the fluid molecular viscosity. For the atmospheric circulation, it is necessary that this ratio must be much larger than 1 to ensure the correct description of the number of cells in the ZSC, which is consistent with the conclusion about the role of eddy viscosity in maintaining the ZSC as discussed in Pedlosky.[29]

We should emphasize that the above result regarding the number of cells is obtained simply as a consequence of the PES condition for the governing system (2.1). In the real atmosphere, (2.1) is certainly too idealized, as we have not accounted for a lot of detailed atmospheric physics. However, the fact that (2.1) could expose the typical behaviors of the dynamical transition indicates that the existence of the triple-cell structure of the ZSC likely roots in the intrinsic dynamical nature of the fluid system confined by the scales specific to the Earth's atmosphere. With the same mechanism, it is possible that a different number of large-scale cells may emerge in different planets where these scales are different.

Two issues beyond the count of the number of cells for the ZSC remain. The first issue is related to the structure of the flow after the dynamical transition takes place. It is of importance to see the explicit structure of this new steady-state solution, as the PES condition itself does not indicate how the new steady state looks like. Second, it is critical that any new steady-state solution has to be stable so that the ZSC can be maintained over a long time. An unstable state after the transition would render any new state meaningless for all practical purposes.

C. Structure of the ZSC

With the PES condition for the dynamical transition to occur as demonstrated in the preceding section, our next task is to derive an expression for the new states that the system will bifurcate to. According to the PES condition, the new steady state is nothing but the first eigenstate corresponding to the first eigenvector λ_1. Because of the fundamental role of the Coriolis force, we will consider the structure of the atmospheric circulation for two different cases.

1. No Coriolis force

Because the dynamical transition concerns with the first eigenvector, let us denote the first eigenvector as ϕ_1, which has the following form at $R = R_0$:

$$\phi_1 = \begin{pmatrix} \frac{-T\pi C_1}{P_r G_{1,1}} \sin b_1 y \cos \pi z \\ -C_1 \sin b_1 y \sin \pi z \\ \frac{(1-B)b_1 C_1}{G_{1,1}} \cos b_1 y \sin \pi z \end{pmatrix}, \tag{3.17}$$

where the explicit value $m_0 = 1$ has been used in the absence of the Coriolis force, and the amplitude C_1 is obtained from the normalized condition as (see Appendix B)

$$C_1 = \frac{2}{\sqrt{(P_r + 1)aA_{1,1}}}.$$

To find an expression for the eigenvectors in the neighborhood of R_0, we recall that the steady state given by (2.3) is stable if $R < R_0$. For R is larger but still sufficiently close to R_0, (2.7) is however reduced to a set of ordinary equations on the central manifold around the first eigenvectors (B9) at the critical value R_0. Detailed derivations of the eigenfunctions on this central manifold spanned by these first eigvenvectors at $R = R_0$ show that for $R > R_0$ (2.7) bifurcates to an attractor consisting of two new steady states $\{\varphi_1, \varphi_2\}$. Detailed analysis of these new state requires additional analysis on the central manifold with the full nonlinear terms included. The nonlinear analysis needed to derive the approximated structure of the solution near the critical point is given in Appendix C, which results in an expressions for the new steady states on the central manifold are given as follows:

$$\begin{aligned} \varphi_1 &\approx \left(\frac{-\lambda_1}{G(\phi_1, \Psi_1), \phi_1^*)} \right)^{\frac{1}{2}} \phi_1, \\ \varphi_2 &\approx -\left(\frac{-\lambda_1}{G(\phi_1, \Psi_1), \phi_1^*)} \right)^{\frac{1}{2}} \phi_1. \end{aligned} \tag{3.18}$$

where operator G is a bilinear mapping defined as

$$G(\phi_1, \Psi_1) = \begin{pmatrix} J(\phi_{12}, \Psi_{11}) \\ J(\phi_{12}, \Delta\Psi_{12}) \\ J(\phi_{12}, \Psi_{13}), \end{pmatrix} \tag{3.19}$$

with Ψ_1 given by (see the derivation of (3.18) in Appendix C)

$$\Psi_1 = \begin{pmatrix} \Psi_{11} \\ \Psi_{12} \\ \Psi_{13} \end{pmatrix} = \begin{pmatrix} \frac{-TC_1^2\pi^2 b_1}{2G_{1,1}(2\lambda_1+4Eb_1^2)} \sin 2b_1 y \\ 0 \\ \frac{-\pi(1-B)\pi C_1^2 b_1^2}{2G_{1,1}(2\lambda_1+4\pi^2)} \sin 2\pi z \end{pmatrix}.$$

The existence of these two stable steady states φ_1, φ_2 is important, as it implies two opposite directions for the general atmospheric circulations in two Hemispheres. To see the implication of these new steady states in more details, we recall that the first component of the eigenvectors φ_i, $i = 1, 2$ describes the zonal motion in x-direction, the second component describes the streamfunction on the (y, z)-plane, and the third component corresponds to temperature perturbation θ. Explicit calculations of all wind components from the streamfunction and temperature corresponding to the first eigenvector φ_1 is

$$\begin{pmatrix} u(y,z) \\ v(y,z) \\ w(y,z) \\ \theta(y,z) \end{pmatrix} = \begin{pmatrix} 0 \\ -\Gamma_1\pi \sin\frac{\pi y}{a} \cos\pi z \\ \frac{\Gamma_1\pi}{a} \cos\frac{\pi y}{a} \sin\pi z \\ \Upsilon_1 \cos\frac{\pi y}{a} \sin\pi z + \frac{\theta_1}{\theta_1-\theta_2} - z \end{pmatrix}, \tag{3.20}$$

where the parameter $T = 0$ has been used in the u component due to $f = 0$, and two amplitudes Γ and Υ are defined as

$$\Gamma_1 = \left(\frac{-\lambda_1}{G(\phi_1, \Psi_1), \phi_1^*)}\right)^{\frac{1}{2}} C_1,$$

$$\Upsilon_1 = \left(\frac{-\lambda_1}{G(\phi_1, \Psi_1), \phi_1^*)}\right)^{\frac{1}{2}} \frac{(1-B)b_1 C_1}{G_{1,1}}.$$

There are several noteworthy properties about the steady state φ_1 that can be immediately seen from (3.20). First, one notices that (3.20) represents indeed a single-cell circulation with a northerly wind ($v < 0$) in the lower half of troposphere (i.e., $z < 0.5$) and a southerly wind in the upper half of the troposphere. Corresponding to this meridional flow is an ascending motion in the equator and a descending motion in the pole. This large-scale circulation is expected for a thermally direct cell circulation, as the warmer air tends to flow towards the polar region at the upper level, descends and returns back to the equator near the surface as constrained by the north-south temperature gradient (see Figure 2)

Given the aspect ratio of the horizontal to the vertical scales of the ZSC $a = L/H \sim 10^3$, it can be further seen from (3.20) that the ratio $w/v = H/L \sim 10^{-3}$, which is again consistent with the observation that the vertical motion is roughly 10^{-2} ms^{-1}, while the horizontal wind is ~ 10 ms^{-1}. In addition to this single-cell meridional structure, it is also seen that the zonal wind u is strictly zero everywhere, and so the ZSC must be entirely confined within the (y, z) plane in the absence of the Coriolis force. In this regard, the ZSC is simply a pure thermal direct cell with no zonal circulation. Such a single-cell structure could maintain the heat balance between the equator and the pole, while on the other hand ensure the conservation of the absolute angular momentum.[21,39]

Of further interest is that the physical requirement of the north-south temperature gradient with a warmer equator than the polar regions breaks the symmetry between the two-state attractor φ_1 and φ_2 in each hemisphere. Recall that the

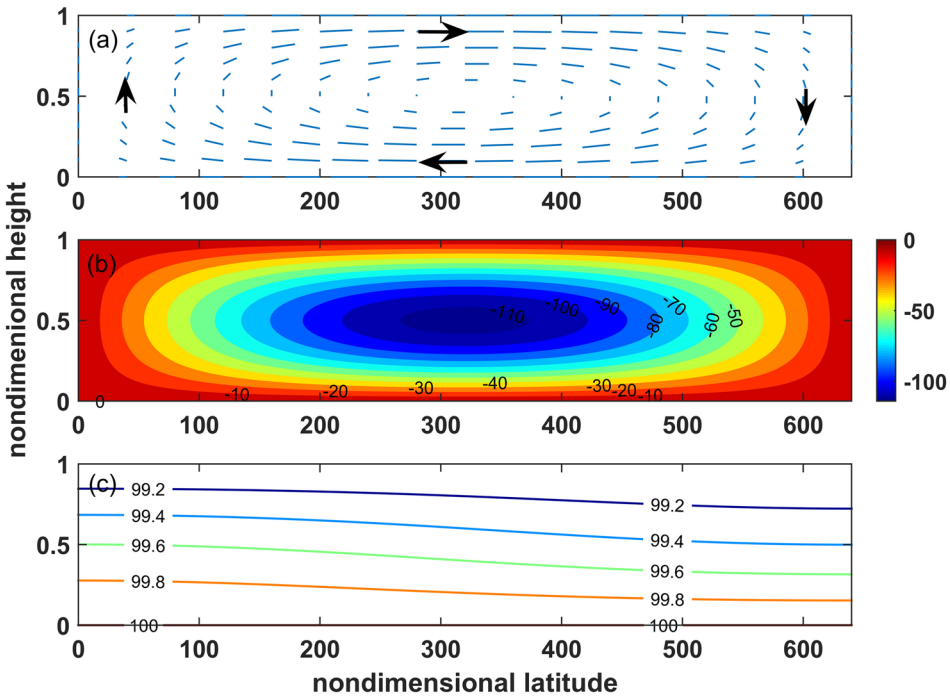

FIG. 2. (a) Vertical cross section of the (v, w) components in the (z, y) plane after the dynamical transition takes place when $R > R_0$ in the absence of the Earth's rotation; (b) the streamfunction, and (c) the total temperature as obtained from the analytical solution (3.20), assuming the following scales: $\theta_1 = 300\ K$, $\theta_2 = 297\ K$, $H = 10\ km$, $\kappa_2 = 100\ m^2\ s^{-1}$, Prandtl number $P_r = 1$, and the diabatic heating coefficient $\zeta = 10^{-4}\ K\ s^{-1}$.

components for the second eigenvector φ_2 differs from those in φ_1 only by the minus sign as seen in (3.18). Such a difference turns out to be important, because it indicates that the temperature gradient will be oriented towards the equator for φ_2, i.e., warmer in the poles and colder in the equator. A reverse temperature gradient for the steady state φ_2 means φ_2 is an unphysical solution in the Northern Hemisphere, and is apparently not consistent with the actual temperature gradient in the atmosphere. In the Southern Hemisphere, it is noted, however, that $T \sim f < 0$. Thus, it is now the solution φ_2 that has the right structure of the large-scale circulation in the Southern Hemisphere, because it could maintain not only the right circulation orientation in the meridional plane, which is opposite to that in the Northern Hemisphere, but also ensure the correct temperature gradient direction from the equator to the pole as expected.

2. With Coriolis force

In the presence of the Earth rotation with $f \neq 0$, the structure of the large-scale circulation changes dramatically. Following the same procedure as for the case of $f = 0$ in the preceding subsection, we obtain the following steady state in the Northern Hemisphere for $f \neq 0$:

$$\begin{pmatrix} u(y,z) \\ v(y,z) \\ w(y,z) \\ \theta(y,z) \end{pmatrix} = \begin{pmatrix} -\frac{T\pi\Gamma_3}{P_r G_{3,1}} \sin\frac{3\pi y}{a} \cos\pi z. \\ -\Gamma_3\pi \sin\frac{3\pi y}{a} \cos\pi z \\ \frac{3\Gamma_3\pi}{a} \cos\frac{3\pi y}{a} \sin\pi z \\ \Upsilon_3 \cos\frac{3\pi y}{a} \sin\pi z + \frac{\theta_1}{\theta_1-\theta_2} - z \end{pmatrix}, \tag{3.21}$$

where the amplitudes are

$$\Gamma_3 = \left(\frac{-\lambda_1}{(G(\phi_1,\Psi_1),\phi_1^*)}\right)^{\frac{1}{2}} C_3, \quad C_3 = \frac{2}{\sqrt{(P_r+1)aA_{3,1}}},$$
$$\Upsilon_3 = \left(\frac{-\lambda_1}{G(\phi_1,\Psi_1),\phi_1^*)}\right)^{\frac{1}{2}} \frac{(1-B)b_3C_3}{G_{3,1}}, \tag{3.22}$$

We note that that above expression for the eigenvectors near the critical point R_0 is under an approximation that $0 < \frac{R-R_0}{R} \ll 1$, i.e. the Rayleigh number has to be sufficiently close to its critical value (see Appendix C). A larger value of R would require high-order contributions from the nonlinear terms that are unnecessarily complex for our analyses. A closer examination of this solution shows several more interesting features than the case of $f = 0$. First, in terms of the meridional circulation (v, w), it can be explicitly seen now that there exist three different cells as illustrated in Figure 3, with the vertical motion w much less than the meridional wind component v as expected.

Along with this triple-cell structure, it is of particular interest to note that the zonal wind shows a consistent pattern at the surface with an easterly wind for the first cell, followed by a westerly flow for the second cell, and finally easterly flow again for the third cell (Figure 4). These alternative easterly and westerly winds accord well with the observed surface wind distribution related to the Hadley, the Ferrell, and the Polar cells. At the upper troposphere $z > 1/2$, the zonal wind changes its directions and exhibits a westerly jet for the first cell, albeit its magnitude is not comparable to that of the

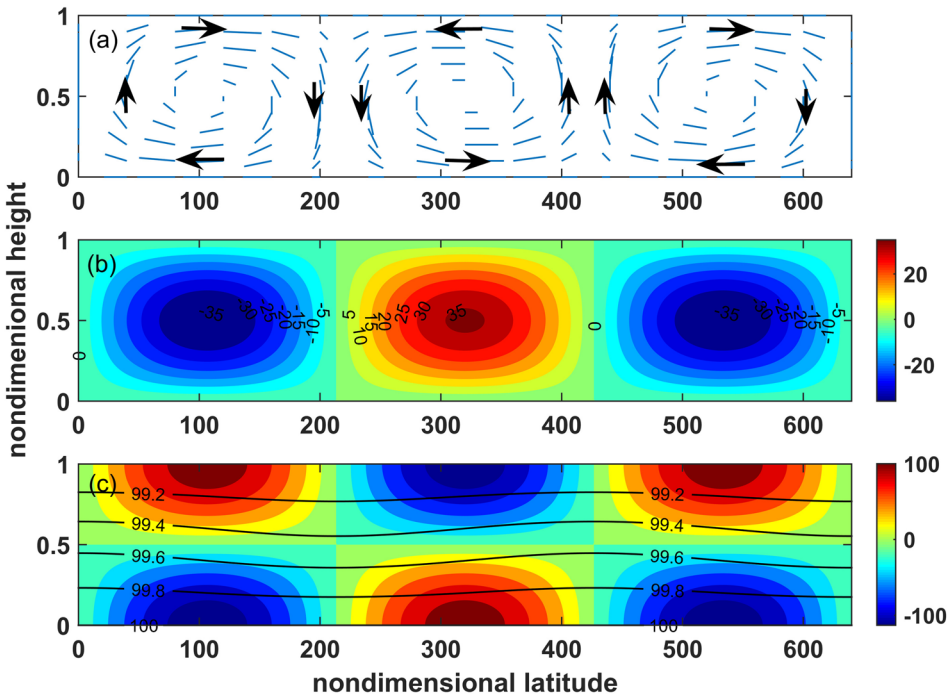

FIG. 3. Similar to Figure 2 but for the meridional circulation given by (3.21) in the presence of the Coriolis force, assuming the same set of parameters and $f = 10^{-5}\ s^{-1}$.

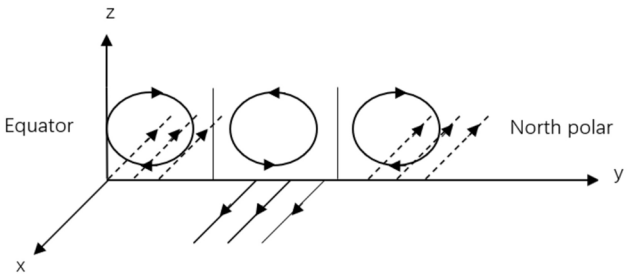

FIG. 4. Three-dimensional illustration of the zonally symmetric circulation in the presence of the Coriolis force after the transition takes place when $R > R_0$. The illustration is drawn from the stable steady state φ_1 given by (3.21) in the Northern Hemisphere. Vectors denote the zonal wind at the surface.

real upper-level easterly jet around 35N. Such a specific pattern of the zonal and meridional winds in this first cell is again consistent with the flow structure of the Hadley circulation. Likewise, the second and the third cells are also naturally consistent with Ferrell and Polar circulations as observed. One can see here the importance of the vertical eddy term in maintaining these cell structures similar to the Rayleigh-Beńard convective cells.

That these results are obtained directly from the governing equation (2.1) reveals an interesting fact that the key characteristics of the ZSC appear to be understood within the framework of the dynamical transition on the f-plane. Unlike modeling studies that contain many internal feedbacks that are often hard to understand how the development of the three-cell structure of the atmospheric general circulation takes place, our analytical model provides a condition for such a structure to happen, which is well applied to the Earth's atmosphere. Specifically, the nondimensional number $R \equiv gH^3(\theta_1 - \theta_2)/\theta_0\kappa_2^2$ has to be larger than a critical value R_0, which is $\sim 8 \times 10^8$ as can be directly estimated from (3.12). Given $H \sim 10^4$ m, $\theta_0 \approx 300$ K, $\kappa_2 \approx 10$ m^{-1}, this condition on R_0 imposes that the difference in temperature between the top and the surface layer $\Delta\theta = \theta_1 - \theta_2$ must be larger than ~ 2.5 K so that the PES condition can be realized. This requirement is indeed well applied to the equivalent potential temperature difference in the real atmosphere. Physically, this condition just reiterates that the temperature difference between the surface and the tropopause must be sufficiently large so that large-scale thermal cells can emerge, similar to Rayleigh-Bénard convection.

Regarding the ZSC in the Southern Hemisphere, it should be remarked that all of the aforementioned discussions about the ZSC structure and transition can be well applied, using the other steady state φ_2. Indeed, in the Southern Hemisphere for which the nondimensional number $T \sim f < 0$, the zonal flow is still the same as that in the Northern Hemisphere, because the function $\sin(3\pi y/a) < 0$ for $y < 0$. Thus, there is no net change in the sign of the zonal flow (see the u component in (3.21)). On the other hand, the meridional circulation will have its orientation reversed, because the sign of the vertical motion is unchanged whereas the meridional wind changes its sign due to the $\sin(3\pi y/a)$ function. As such, the flow structure for both the zonal and the meridional circulations are consistent with observations in the Southern Hemisphere as expected.

D. Stability of the ZSC

The last important issue concerns the stability of the ZSC structure obtained in the previous section. To prove the stability of the steady state φ_1 for the Northern Hemisphere and φ_2 for the Southern Hemisphere, we use Ma and Wang's structural stability theorem[25] for a 2D divergence-free vector field to show that this new state is structurally stable. To be specific, we will demonstrate the stability proof for case of $f = 0$. The other case of $f \neq 0$ can be proven in very similar way (see Appendix C).

Recall that the necessary and sufficient conditions for the structural stability of a 2D divergence-free vector field $\mathbf{u} \equiv (v, w)$ as established in Ma and Wang[25] (see Chapter 4) are

1. (v, w) must be regular, i.e., $\det(J(\mathbf{u})) \neq 0$.
2. All interior saddle points of $\mathbf{u}$ are self-connected.
3. Each boundary saddle point is connected to a saddle point by the same connected component of boundary.

Because there is no saddle point for the steady state φ_1, the last two conditions are trivial. Hence, all we have to do is to simply check for the regularity property of the flow field (v, w) associated with φ_1. Indeed, a straightforward calculation of the Jacobien of the flow field $\mathbf{u} = (v, w)$ then gives

$$\det(\mathbf{J}(\mathbf{u})) = \begin{vmatrix} -\frac{\Gamma_1\pi^2}{a}\cos\frac{\pi y}{a}\cos\pi z & -\Gamma_1\pi^2\sin\frac{\pi y}{a}y\sin\pi z \\ -\frac{\Gamma_1\pi^2}{a^2}\sin\frac{\pi y}{a}y\sin\pi z & \frac{\Gamma_1\pi^2}{a}\pi\cos\frac{\pi y}{a}y\cos\pi \end{vmatrix}$$
$$= -\frac{\Gamma_1^2\pi^4}{a^2}\left(\cos^2(\frac{\pi y}{a}y)\cos^2(\pi z) + \sin^2(\frac{\pi y}{a}y)\sin^2(\pi z)\right) < 0, \tag{3.23}$$

which implies that $\mathbf{u}$ is a D-regular vector field. Clearly, $\mathbf{u}$ does not contain any interior saddle points and ∂-saddle points. Thus, Ma and Wang's stability theorem holds true, and the new state given by φ_1 as shown in Fig. 2 is topologically stable. Because this method can be well applied in both the presence and in the absence of the Earth's rotation, we conclude that both structures shown in Fig. 2 and Fig. 3 are stable, thus justifying the persistent existence of the triple-cell structure for the atmospheric general circulation in the presence of the Earth's rotation.

IV. APPLICATION TO THE ATMOSPHERIC GLOBAL CIRCULATIONS

While the ZSC model presented in this study could capture some interesting behaviors of the zonally symmetric structure with a single cell in the absence of the Earth's rotation and a 3-cell structure in the presence of the Earth's ration, a number of major simplifications in this model raise several

questions about the possible application of the ZSC model to the real atmospheric general circulation.

For the case without the Coriolis force ($f = 0$), the result obtained from our ZSC model can be in fact compared to previous theoretical and modelling studies of the zonally symmetric global circulation with fixed sea surface temperature.[13,31,33,35,37,41] One of the most common feature in all of these previous studies of the zonal symmetric circulation is the existence of one single-cell circulation in each hemisphere in the absence of Earth's rotation. For example, the idealized simulation in Ref. 33 showed a dominant cell as a result of radiative-convective instability, which is very sensitive to the cloud absorption parameter. Likewise, the three-dimensional simulations on an aqua-planet with fixed surface temperature in Refs. 31 and 35 captured also a single-cell structure in each hemisphere (see, e.g., Figure 1 in Reed et al.[35]).

Due to various setting and configurations in these models, one notices that the single-cell structure obtained from these studies has somewhat different sizes and strength. In the study of Raymond,[33] the horizontal scale of a moisture anomaly imposed at the initial time is limited to a region of 2000 km wide and it is placed about 5 degree north of the Equator to mimic the location of the ITCZ during the summer time in the Northern Hemisphere. As a result, the single-cell circulation obtained from this simulation is confined within the a region of 30S-30N instead of expanding all the way to the poles. In contrast, the meridional extent of the single-cell circulation in other studies[31,35,37] is much larger than those in the Raymond's simulation, which could reach as far as ~60S-65N. Of course, this comparison is not fully justified, as some simulations were based on a three-dimensional model,[31,35] whereas the two-dimensional zonally symmetric configuration was used in other simulations.[33,37] Nonetheless, the dominance of a single-cell structure in all of these modelling studies in the absence of the Earths rotation to some extent supports the analytical result obtained from our ZSC model as well as Farrells early conjecture in the limit of inviscid flows.[7]

Regarding the case with the Coriolis effects taken into account, the interpretation of the 3-cell structure derived from our ZSC model as the classical Hadley, Ferrel, and Polar cells is far more nontrivial and must be examined with cautions. While the nature of the Hadley cell as a consequence of the thermal direct circulation is plausibly captured by one of the cells in the ZSC model, the identification of the second cell in our ZSC model as the Ferrel cell is much harder to convince. This is because the Ferrel cell has been well known to be a thermally indirect circulation as a result of the eddy momentum and heat flux convergences.[3,13,30,40,41] In the diagnostic framework based on the Kuo-Eliassen equation for the mass streamfunction, it can be demonstrated that both the eddy heat flux and the eddy momentum flux could offset the direct diabatic forcing at midlatitudes, thus driving mean meridional cells in each hemisphere with rising motion poleward of 45° and sinking motion equatorward of 45°. Note that these large-scale eddy flux convergences cannot be independently prescribed, but they must respect both the force balance for the eddy momentum flux convergence and the baroclinic heat transfer balance for the eddy heat flux.[3,13]

In our ZSC model, the emergence of the second thermally indirect cell comes naturally from the governing equations, much like convective cells in Reynold-Bénards convection. Physically, the appearance of the thermally indirect cell can be understood as a combination of the Coriolis force, the thermal equation, the continuity equation, and the eddy terms in Eq. (2.1). As the Coriolis force is allowed, the poleward wind component of the first cell at the upper level will be soon deflected to the east and eventually descend due to its cooler temperature at the upper level, forming the descending of the Hadley cell. This descending motion will reach the surface around 30N and spread out as a consequence of the continuity equation and boundary condition, generating two branches of the surface wind at 30N; one returns to the Equator, and the other moves to the pole. The poleward component at the surface, which is now a part of the surface flow of the second cell, will become warmer due to its interaction with the surface and at some point must raise, thus forming the upward branch of the Ferrel cell. Without the Earth rotation, the upper branch of the first cell can continue all the way to the pole before descending due to the absence of the Coriolis acceleration in the zonal direction. From this perspective, the Coriolis effect intuitively makes a big difference in the zonally symmetric global circulation.

In the above physical interpretation, the importance of the large-scale eddy momentum fluxes is implicitly encoded in the eddy term $\nu_2 \frac{\partial^2 v}{\partial z^2}$ and the boundary conditions, which ensures that the meridional flows must be always maximum at the surface and the top boundary. As such, the v component has to decrease with height so that $\nu_2 \frac{\partial^2 v}{\partial z^2}$ is positive in the lower half and negative in the upper half of the troposphere. This negative eddy-induced acceleration at upper half of the troposphere means that the upper branch of the Ferrel cell must turn towards the Equator in the 30N-60N region as would expected from the classical eddy momentum flux convergence. In this regard, the term $\nu_2 \frac{\partial^2 v}{\partial z^2}$ in our ZSC model should not be interpreted as a diffusion term, but more as a parameterization of the large-scale eddy momentum fluxes that are often written in the form of eddy stress $\frac{\partial(\overline{v'w'})}{\partial z}$, and similarly for the eddy heat flux. Of course, this interpretation may not account for the zonal drag term, which could enhance substantially the strength of the Ferrel cell as demonstrated in Ref. 3. However, the fact that a thermally indirect cell can develop in the ZSC model confirms that the role of the eddy momentum and heat fluxes is critical. The thermally indirect cell obtained from the ZSC model in this regard proposes a mechanism for the Ferrel cell that is similar to the convective cells in the Reynolds-Bénard problem.

Our above interpretation of the 3-cell structure in the ZSC model by no mean indicates that the ZSC model can realistically describe the Earth's atmospheric general circulations due to various simplifications and approximations. Among

these simplifications, the simple diabatic heating approximation in terms of vertical motion given by Eq. (2.2) is perhaps the most severe drawback, which limits the applicability of the ZSC model to the real atmosphere. While this parameterization of the diabatic heating is reasonable in the tropical region, it implies however that the equivalent potential temperature anomaly is positive the midlatitude region (i.e., a warmer anomaly in the ascending branch of the Ferrel cell) than in the subtropical region (i.e., a colder anomaly in the descending branch of the Ferrel cell) as seen in Figure 3c. Of course, the realistic surface temperature has a large negative gradient such that the tropical region is always much warmer than the polar region, and so a warmer anomaly does not necessarily mean an overall warmer total temperature. Nevertheless, a warmer anomaly in the midlatitude atmosphere as compared to the subtropical atmosphere is difficult to verify, because there is no reference atmospheric temperature with no atmospheric circulations so that the temperature anomaly associated with the thermally indirect cell can be calculated and validated.

Second, our investigation of the ZSC structure in this study is based on the nonlinear analyses on the central manifold, instead of using the traditional approaches that linearize the model state around a given steady solution as in previous studies of general atmospheric circulations. An expense for such a rigor in our model is the sacrifice of few important properties of the real atmospheric circulation such as the variation of the tropospheric depth with latitude, the detailed moist processes, the cloud-radiative feedbacks, the curvature effects of the Earth's surface, the β effects, the atmospheric boundary layer processes, or the Rhines scales. In this sense, our model is more appropriate in the laboratory setting with a rotating tank.[15] Such shortcomings are to a large extent unavoidable for any analytical model, which would be otherwise buried due to the complicated nonlinearity of the Navier-Stokes equations.

V. CONCLUSION

In this study, an f–plane dynamical model for incompressible flows was proposed to understand the structure and stability of the zonally symmetric circulation (ZSC). The fundamental questions that we wish to address here are 1) whether the ZSC possesses a triple-cell structure similar to the Hadley, Ferrel, and Polar cells in the Earth's global atmospheric circulations, 2) does the ZSC accept a single-cell structure in the absence of the Coriolis force as previously hypothesized?, and 3) what is the condition for the triple-cell structure to emerge as a consequence of the Earth's rotation? In addition to these questions, it is of importance to examine also the stability of these single-cell and triple-cell structures such that these structures can represent a real configuration of the atmospheric circulations.

Using the dynamical transition framework developed by Ma and Wang, it was found that the incompressible Navier-Stokes equations under the zonally symmetric configuration could naturally support intricate structures of the ZSC similar to those in the global atmospheric circulations, even within the f–plane dynamics. Specifically, two findings were obtained as a result of the Principle of Exchange of Stabilities (PES) condition in the absence of the Coriolis force: i) there exists a single circulation similar to the single-cell structure from the equator to the pole in response to the warmer tropical region and a colder pole region as previously hypothesized, and ii) there is no zonal wind. Physically, this result implies that the ZSC will be completely confined in the meridional plane if the Coriolis effects are not accounted, which is consistent with laboratory tank experiments.[15]

In the presence of the Coriolis force, detailed analyses of the PES condition showed that the Coriolis force is indeed a critical parameter for the triple-cell structure of the ZSC. The most direct effect is that the Coriolis force allows for a transition to a new steady state consisting of exactly three cells, provided that the rotation rate, the horizontal and vertical eddy viscosity coefficients, and the vertical temperature gradient between the surface and the top boundary satisfy a certain constraint. The new steady state emerged as a result of the dynamical transition displays all essential features of the realistic global atmospheric circulations including the triple-cell structure, the easterly zonal surface wind in the tropical region, the westerly zonal surface wind in the midlatitude, and the easterly zonal surface wind in the polar region. The drastic difference in the magnitude of the vertical and horizontal winds is also well reflected, despite the simplified physics and diabatic heating parameterizations in our model.

It is of interest to note that the topology of the ZSC structure in our model does not appear to depend upon the specific functional form of the diabatic heating parametrization, but more on the rotation rate, the scale of the Earth's atmosphere, the vertical temperature gradient, and the ratio of the horizontal to the vertical momentum eddy coefficients. Unlike the traditional model for the general circulation, our ZSC model shows that the vertical temperature gradient and the scale ratio of the fluid layer are among the key factors in determining the structure of the ZSC. Furthermore, a ratio between the horizontal and the vertical eddy coefficients $\frac{\nu_1}{\nu_2} \sim 10^5$ is required to allow for three but not an arbitrary number of cells. Such a vital role of the momentum eddy coefficients in maintaining the ZSC structure was in fact well perceived in early studies,[29,39] but not yet fully proven. In this regard, our model could explicitly highlight the roles of the large-scale eddy coefficients in the real Earth's atmosphere consistent with previous studies.

Given the drawbacks in our model, it is apparent that the ZSC model will not provide satisfactory explanation for several essential aspects of the general atmospheric circulations including moist radiative-convective equilibrium, baroclinic zonal jets, Rhines scale cascade, or the size of the general atmospheric circulations cells.[5,34,36,43] As such, the interpretation of our results should be confined to a simple context of the three questions stated above. That is, we wish to explore to the maximum extent how the zonally symmetric dry f–plane dynamics can allow us to capture the main

structure and stability properties of the general atmospheric circulations as observed. On the other hand, the exact nature of the results presented in this study brings some insights into why the general atmospheric circulations possesses triple-cell structure but not four or five cells. In addition, we have obtained a criterion for such a triple-cell structure to exist, which depends sensitively on the Earth's rotation rate, the ratio of vertical over horizontal momentum eddy coefficients, the scales of the Earth's atmosphere, and the vertical temperature gradient. From this perspective, our study complements the observational and modeling studies of the general atmospheric circulations by providing alternative insights into the characteristics of the atmosphere, and explains the well-observed structure of the Earth's general atmospheric circulations.

ACKNOWLEDGMENTS

This research is supported in part by the Indiana University Grand Challenge Research fund, and by the Office of Naval Research (ONR)'s Young Investigator Program Award. We wish to thank two anonymous reviewers for their constructive comments and suggestions, which have helped improve the presentation of this work substantially.

APPENDIX A: CRITICAL RAYLEIGH NUMBER

In Eq. (3.10), it is clear that λ is proportional to R, and for $R = +\infty$, $\lambda > 0$ is always true. Thus, there must exist $R = R_{mn} > 0$ such that $\lambda = 0$. In fact, one can derive from the condition $\lambda = 0$ that

$$R_{mn} = \frac{P_r^2 G_{m,n}^2 A_{m,n} + T^2 n^2 \pi^2}{P_r (1-B) b_m^2}, \tag{A1}$$

which increases with n. Let

$$R_0 = \min_{m \geq 1, n=1} R_{mn}, \tag{A2}$$

and observe that only $b_m = \frac{m\pi}{L}$ contains m in R_{m1}. All other terms are constant. Thus, let b_m^2 as x. Then R_0 is the minimum value of the following function

$$F(x) = \frac{P_r^2 \left(\pi^2 + Ex\right)^2 \left(\pi^2 + x\right) + T^2 \pi^2}{P_r (1-B) x}.$$

One notices that the function $F(x)$ has following properties:

$$\begin{aligned} &F(x) \to +\infty, \text{as} \quad x \to 0^+, \\ &F(x) \to +\infty, \text{as} \quad x \to +\infty, \\ &F(x) > 0, \text{for any} \quad x \in (0, +\infty). \end{aligned}$$

These properties yield that $F(x)$ must have a minimum value in $(0, +\infty)$, which is determined by $F'(x) = 0$, i.e.,

$$x^3 + \left(\frac{\pi^2}{2} + \frac{\pi^2}{E}\right) x^2 - \frac{P_r^2 \pi^6 + T^2 \pi^2}{2 P_r^2 E^2} = 0.$$

If the positive zero of preceding equation is very small, we can obtain an approximate value for x_T as follows:

$$b_m^2 \equiv x_T \approx \sqrt{\frac{P_r^2 \pi^4 + T^2}{P_r^2 (E^2 + 2E)}}.$$

which is Eq. (3.13) in the main text. Apparent, if Coriolis force is neglected, the above expression for x_T will reduce to

$$b_0^2 \equiv x_0 \approx \frac{\pi^2}{\sqrt{(E^2 + 2E)}}.$$

APPENDIX B: THE FIRST EIGENVECTOR AT CRITICAL RAYLEIGH NUMBER R_0

It is known from (3.3) that its first eigenvector can be expressed in a separable form. For convenience in determining transition number in foregoing section, it is necessary to get exact expression of this first eigenvector. From Eqs. (3.4), (3.8), and (3.9) in the main text, one can easy see that the second component of the first eigenvector at R_0 is

$$\psi = -A \sin b_{m_0} y \sin n\pi z, \tag{B1}$$

with which one obtains other fields

$$u = \frac{-T\pi A}{P_r G_{m_0,1}} \sin b_{m_0} y \cos \pi z, \tag{B2}$$

$$\theta = \frac{(1-B) A b_{m_0}}{G_{m_0,1}} \cos b_{m_0} y \sin \pi z. \tag{B3}$$

Following a similar approach as in the main text, the dual eigenvalue problem of (3.3) is then easily obtained as:

$$\begin{aligned} &P_r \left(E \frac{\partial^2 u^*}{\partial y^2} + \frac{\partial^2 u^*}{\partial z^2}\right) + T \frac{\partial \psi^*}{\partial z} = \lambda u^*, \\ &P_r \left(E \frac{\partial^2 \Delta\psi^*}{\partial y^2} + \frac{\partial^2 \Delta\psi^*}{\partial z^2}\right) - T \frac{\partial u^*}{\partial z} + (1-B) \frac{\partial \theta^*}{\partial y} = \lambda \Delta\psi^*, \\ &K \frac{\partial^2 \theta^*}{\partial y^2} + \frac{\partial^2 \theta^*}{\partial z^2} + R \frac{\partial \psi^*}{\partial y} = \lambda \theta^*. \end{aligned} \tag{B4}$$

The dual eigenvalue problem (B4) is introduced here so that the orthogonal property is ensured, i.e. $(u, \psi, \theta) \cdot (u^*, \phi^*, \theta^*)^T \neq 0$ if the eigenvalue λ corresponding to (u, ψ, θ) is conjugate to that of (u^*, ψ^*, θ^*), and $(u, \psi, \theta) \cdot (u^*, \psi^*, \theta^*)^T = 0$ otherwise. This orthogonal property is required to derive the corresponding reduced equation on the central manifold (see more details in Ref. 25).

It can be now seen that the dual eigenvalue problem (B4) leads to a set of relationships for $U^*(z)$, $V^*(z)$ and $W^*(z)$, which satisfy the following dual system

$$\begin{aligned} &P_r \left(D^2 - E b_m^2\right) U^* + T D V^* = \lambda U^*, \\ &P_r \left(D^2 - E b_m^2\right) (D^2 - b_m^2) V^* - T D U^* \\ &\quad = \lambda (D^2 - b_m^2) V^* - (1-B) b_m W^* \\ &\left(D^2 - K b_m^2\right) W^* - R b_m V^* = \lambda W^*, \\ &\text{Boundary: } U^{*'} = V^* = V^{*''} = W^* = 0, z = 0, 1, \end{aligned} \tag{B5}$$

As a result, one can get the dual first eigenvector as follows

$$u^* = \frac{T\pi A}{P_r G_{m_0,1}} \sin b_{m_0} y \cos \pi z, \tag{B6}$$

$$\psi^* = A \sin b_{m_0} y \sin \pi z, \tag{B7}$$

$$\theta^* = \frac{R b_{m_0} A}{G_{m_0,1}} \cos b_{m_0} y \sin \pi z. \tag{B8}$$

To finally determine the amplitude A of the first eigenvector $\phi_1 \equiv (u, \psi, \theta)^T$ and the corresponding dual eigenvector $\phi_1^* \equiv (u^*, \psi^*, \theta^*)^T$, we recall the normalization condition given by

$$(\mathcal{A}\phi_1, \phi_1^*) = 1.$$

Direct calculation of this condition thus results in

$$\phi_1 = \begin{pmatrix} \frac{-T\pi C_{m_0}}{P_r G_{m_0,1}} \sin b_{m_0} y \cos \pi z \\ -C_{m_0} \sin b_{m_0} y \sin \pi z \\ \frac{(1-B) b_{m_0} C_{m_0}}{G_{m_0,1}} \cos b_{m_0} y \sin \pi z \end{pmatrix}, \tag{B9}$$

$$\phi_1^* = \begin{pmatrix} \frac{T\pi C_{m_0}}{P_r G_{m_0,1}} \sin b_{m_0} y \cos \pi z \\ C_{m_0} \sin b_{m_0} y \sin \pi z \\ \frac{R b_{m_0} C_{m_0}}{G_{m_0,1}} \cos b_{m_0} y \sin \pi z \end{pmatrix}, \tag{B10}$$

where C_{m_0} is given by

$$C_{m_0} = \frac{2}{\sqrt{(P_r + 1) a A_{m_0,1}}}.$$

APPENDIX C: THE REDUCED EQUATION

It is well known that the transition of problem (3.10) at critical values R_0 with specified parameters T, E and P_r is well described by its reduced equations on the associated with central manifold. On the central manifold, the partial differential equations can be reduced into a ordinary equations which bring convenience to study of transition from one state to another state. Denote the central space as H_c which is span of all first eigenvectors, i.e. for any element ϕ in H_c can be expressed as

$$\phi = \eta \phi_1. \tag{C1}$$

Using operator G given as (C2) defines a bilinear mapping from $H_1 \times H_1$ to H_2 as follows

$$G(\varphi_1, \varphi_2) = \begin{pmatrix} J(\psi_1, u_2) \\ J(\psi_1, \Delta\psi_2) \\ J(\psi_1, w_2) \end{pmatrix}. \tag{C2}$$

Therefore, it follows preceding expression that

$$G(\phi, \phi) = \eta^2 G(\phi_1, \phi_1). \tag{C3}$$

Straightly computing gives that

$$G(\phi_1, \phi_1) = \begin{pmatrix} \frac{-TC_{m_0,1}^2 \pi^2 b_{m_0}}{2PrG_{m_0,1}} \sin 2b_{m_0} y \\ 0 \\ \frac{-(1-B)\pi C_{m_0,1}^2 b_{m_0}^2}{2G_{m_0,1}} \sin 2\pi z \end{pmatrix}$$

The following derives the expression of central manifold function $h(\phi)$. Let

$$h(\phi) = h_2(\phi) + o(|\eta|^2), \tag{C4}$$

in which h_2 is the quadratic leading order approximation of the center manifold function, which is uniquely determined by the equations

$$2\lambda_1 \mathcal{A} h_2(\varphi) - \mathcal{L} h_2(\varphi) = \mathcal{G}(\varphi, \varphi) = \eta^2 \mathcal{G}(\varphi_1, \varphi_1) \tag{C5}$$

Above equation plays a key role in deriving reduced equation, the process deriving the equation is in section of centre manifold.

Now, let $h_2 = \eta^2 \Psi_1$, then Ψ_1 is determined by

$$2\lambda_1 \mathcal{A} \Psi_1 - L\Psi_1 = G(\varphi_1, \varphi_1). \tag{C6}$$

It is easy to obtain that

$$\Psi_1 = \begin{pmatrix} \frac{-TC_{m_0,1}^2 \pi^2 b_{m_0}}{2PrG_{m_0,1}(2\lambda_1 + 4Eb_{m_0}^2)} \sin 2b_{m_0} y \\ 0 \\ \frac{-\pi(1-B)\pi C_{m_0,1}^2 b_{m_0}^2}{2G_{m_0,1}(2\lambda_1 + 4\pi^2)} \sin 2\pi z \end{pmatrix}$$

Then, on the centre manifold, (3.10) can be reduced to

$$\frac{d\eta}{dt} = \lambda_1 \eta + (G(\phi_1, \Psi_1), \phi_1^*) \eta^3 + o(\eta^3). \tag{C7}$$

Straightly calculation gives

$$G(\phi_1, \Psi_1), \phi_1^*) = \frac{a\pi^4 C_{m_0,1}^4 b_{m_0}^2 (2\lambda_1 + 4\pi^2) T^2}{8APr^2 G_{m_0,1}^2} - \frac{(1-B) a\pi^2 (2\lambda_1 + 4Eb_{m_0}^2) b_{m_0}^4 C_{m_0,1}^4 R_0}{8AG_{m_0,1}^2} < 0,$$

$$A = (2\lambda_1 + 4Eb_{m_0}^2)(2\lambda_1 + 4\pi^2).$$

Then, for

$$R > R_0, \frac{R - R_0}{R} \ll 1, \tag{C8}$$

the dynamical behavior of (3.10) is totally described by (C7). From (C7) one can get that the new steady-state for perturbation equations (3.10) with (C8) is approximately given by

$$\varphi_1 \approx \left(\frac{-\lambda_1}{G(\phi_1, \Psi_1), \phi_1^*)} \right)^{\frac{1}{2}} \phi_1,$$

$$\varphi_2 \approx -\left(\frac{-\lambda_1}{G(\phi_1, \Psi_1), \phi_1^*)} \right)^{\frac{1}{2}} \phi_1.$$

φ_1 is the new state of system (3.10), whose first component describes motion in x-direction, the second component describes structure of flow on (y,z)-plane, and the third component together with θ_c is the new distribution of temperature.

APPENDIX D: STRUCTURAL STABILITY OF CONVECTION STRUCTURE

We provide herein the proof of the stability of the ZSC structure in the case of $f \neq 0$. Similar to the case of $f = 0$, we will use Ma and Wang's structural stability theorem of 2D divergence-free vector field to show that the new large scale convection structure is structurally stable. First, we recall the necessary and sufficient conditions for the structural stability of a 2D divergence-free vector field (v, w) are

1. (v, w) must be regular. Namely, $\det(J(u)) \neq 0$.
2. All interior saddle points of u are self- connected.
3. Each boundary saddle point is connected to a saddle point with same connected component of boundary.

Given these conditions, let' denote

$$D = C_{m_0}\left(\frac{-\lambda_1}{G(\phi_1, \Psi_1), \phi_1^*)}\right)^{\frac{1}{2}},$$

it is then apparent that for $f \neq 0$ and $m_0 = 3$ as discussed in the main text we will have

$$\det(\mathbf{J}(\mathbf{u}_{y,z})) = \begin{vmatrix} -Db_3\pi\cos b_3 y\cos\pi z & -D\pi^2\sin b_3 y\sin\pi z \\ -Db_3^2\sin b_3 y\sin\pi z & Db_3\pi\cos b_3 y\cos\pi \end{vmatrix}$$
$$= -D^2 b_3^2\pi^2\left(\cos^2 b_3 y\cos^2\pi z + \sin^2 b_3 y\sin^2\pi z\right) < 0,$$

which means that

$$\mathbf{u}_{y,z} = \begin{pmatrix} v \\ w \end{pmatrix}$$

is a D-regular vector field. Clearly, $\mathbf{u}_{y,z}$ does not contain any interior saddle points and ∂-saddle points. Following Ma and Wang's Theorem, we can see that the new ZSC structure approximately given by $\mathbf{u}_{y,z}$ is structurally stable as expected.

REFERENCES

[1] Antar, B. N. and Fowlis, W. W., "Baroclinic instability of a rotating Hadley cell," J. Atmos. Sci. **38**, 2130–2141 (1981).
[2] Antar, B. N. and Fowlis, W. W., "Symmetric baroclinic instability of a Hadley cell," J. Atmos. Sci. **39**, 1280–1289 (1982).
[3] Chang, E. K., "Mean meridional circulation driven by eddy forcings of different timescales," J. Atmos. Sci. **53**, 113–125 (1996).
[4] Charney, J. G. and Eliassen, A., "On the growth of the hurricane depression," J. Atmos. Sci. **21**, 68–75 (1964).
[5] Dunkerton, T. J. and Scott, R. K., "A barotropic model of the angular momentum–conserving potential vorticity staircase in spherical geometry," J. Atmos. Sci. **65**, 1105–1136 (2008).
[6] Emanuel, K. A., Neelin, J. D., and Bretherton, C. S., "On large-scale circulations in convecting atmospheres," Q. J. R. Meteorol. Soc. **120**, 1111–1143 (1994).
[7] Farrell, B. F., "Equable climate dynamics," J. Atmos. Sci. **47**, 2986–2995 (1990).
[8] Hart, J. E., "Stability of thin non-rotating Hadley circulations," J. Atmos. Sci. **29**, 687–697 (1972).
[9] Hartmann, D. L., *Global physical climatology*. Academic Press, pp 411 (1994).
[10] Hartmann, D. L., "The atmospheric general circulation and its variability," J. Meteor. Soc. Japan **85B** (2007).
[11] Held, I., "Momentum transport by quasi-geostrophic eddies," J. Atmos. Sci. **32**, 1494–1997 (1975).
[12] Held, I. M. and Hou, A. Y., "Nonlinear axially symmetric circulations in a nearly inviscid atmosphere," J. Atmos. Sci. **37**, 515–533 (1980).
[13] Holton, J., *An Introduction to Dynamic Meteorology*, Academic Press, pp 535 (2004).
[14] Hou, A. Y. and Lindzen, R. S., "The influence of concentrated heating on the Hadley circulation," J. Atmos. Sci. **49**, 1233–1241 (1992).
[15] Illari, L., Marshall, J., and McKenna, W., "Virtually enhanced fluid laboratories for teaching meteorology," Bull. Amer. Meteor. Soc. **98**, 1949–1959 (2017).
[16] Iwayama, T. and Okamoto, H., "Theory of eddy viscosity coefficient for two-dimensional inviscid barotropic fluid," Progress of Theoretical Physics **90**, 1229–1240 (1993).
[17] Kieu, C. Q. and Zhang, D.-L., "An analytical model for the rapid intensification of tropical cyclones," Q. J. R. Meteor. Soc **135**, 1336–1349 (2009).
[18] Kodama, Y., Katsumata, M., Mori, S., Satoh, S., Hirose, Y., and Ueda, H., "Climatology of warm rain and associated latent heating derived from TRMM PR observations," J. Climate **22**, 4908–4929 (2009).
[19] Koschmieder, E. L. and Lewis, E. R., "Hadley circulations on a nonuniformly heated rotating plate," J. Atmos. Sci. **43**, 2514–2526 (1986).
[20] Lindzen, R. S. and Hou, A. V., "Hadley circulations for zonally averaged heating centered off the equator," J. Atmos. Sci. **45**, 2416–2427 (1988).
[21] Lorenz, E. N., "The nature and theory of general circulation of the atmosphere," J. WMO. **218**, 2416–2427 (1965).
[22] Lucarini, V., Blender, R., Herbert, C., Ragone, F., Pascale, S., and Wouters, J., "Mathematical and physical ideas for climate science," Reviews of Geophysics **52**, 809–859, https://doi.org/10.1002/2013rg000446 (2014).
[23] Ma, T., and Wang, S., "Dynamic bifurcation and stability in the rayleigh-benard convection **2**, 159–183 (2004).
[24] Ma, T. and Wang, S., "Rayleigh benard convection: dynamics and structure in the physical space," Communications in Mathematical Sciences **5**, 553–574 (2007).
[25] Ma, T. and Wang, S., *Phase transition dynamics* (Springer, 2014).
[26] Manabe, S., "Climate and the ocean circulation," Mon. Wea. Rev. **97**, 775–805 (1969).
[27] Miller, T. L. and Gall, R. L., "Thermally driven flow in a rotating spherical shell: Axisymmetric states," J. Atmos. Sci. **40**, 856–868 (1983).
[28] Ooyama, K., "Conceptual evolution of the theory and modelling of the tropical cyclone," J. Meteor. Soc. Japan **60**, 369–380 (1982).
[29] Pedlosky, J., *Geophysical Fluid Dynamics*, Second Edition (Springer-Verlag, 1982), p. 619.
[30] Pfeffer, R. L., "Wave-mean flow interactions in the atmosphere," J. Atmos. Sci. **38**, 1340–1359 (1981).
[31] Popke, D., Stevens, B., and Voigt, A., "Climate and climate change in a radiative–convective equilibrium version of ECHAM6," J. Adv. Model. Earth Syst. **5**, 1–14 (2013).
[32] Randall, D. A., *General Circulation Model Development: Past, Present, and Future*, Elsevier, p. 416 (2000).
[33] Raymond, D. J., "The Hadley circulation as a radiative-convective instability," Journal of the Atmospheric Sciences **57**, 1286–1297 (2000).
[34] Read, P. L., Yamazaki, Y. H., Lewis, S. R., Williams, P. D., Wordsworth, R., Miki-Yamazaki, K., Sommeria, J., and Didelle, H., "Dynamics of convectively driven banded jets in the laboratory," J. Atmos. Sci. **64**, 4031–4052 (2007).
[35] Reed, K. A., Medeiros, B., Bacmeister, J. T., and Lauritzen, P. H., "Global radiative-convective equilibrium in the community atmosphere model, version 5," Journal of the Atmospheric Sciences **72**, 2183–2197 (2015).
[36] Rhines, P. B., "Waves and turbulence on a beta-plane," J. Fluid Mech. **69**, 417–443 (1975).
[37] Satoh, M., "Hadley circulations in radiative–convective equilibrium in an axially symmetric atmosphere," J. Atmos. Sci. **51**, 1947–1968 (1994).

[38]Schneider, E. K. and Lindzen, R., "Axially symmetric steady-state models of the basic state for instability and climate studies. Part I. Linearized calculations," J. Atmos. Sci. **34**, 263–279 (1977).
[39]Schneider, T., "The general circulation of the atmosphere," Annual Review of Earth and Planetary Sciences **34**(1), 655–688 (2006).
[40]Stone, P. H. and Branscome, L., "Diabatically forced, nearly inviscid eddy regimes," J. Atmos. Sci. **49**, 355–367 (1992).
[41]Vallis, G. K., *Atmospheric and Oceanic Fluid Dynamics: Fundamentals and Large-scale Circulation*, 1st Edition (Cambridge University Pres), p. 745.
[42]Walker, C. C. and Schneider, T., "Eddy influences on Hadley circulations: Simulations with an idealized GCM," J. Atmos. Sci. **63**, 3333–3350 (2006).
[43]Williams, P. D. and Kelsall, C. W., "The dynamics of baroclinic zonal jets," J. Atmos. Sci. **72**, 1137–1151 (2015).